crystallization communications

Cloning, expression, purification, crystallization and preliminary X-ray crystallographic study of GK0767, the copper-containing nitrite reductase from *Geobacillus kaustophilus*

Yohta Fukuda,[a,b,c] **Taro Tamada,**[c]* **Hideto Takami,**[d] **Shinnichiro Suzuki,**[a] **Tsuyoshi Inoue**[b] **and Masaki Nojiri**[a]*

[a]Department of Chemistry, Graduate School of Science, Osaka University, 1-1 Machikaneyama, Toyonaka, Osaka 560-0043, Japan, [b]Department of Materials Chemistry, Graduate School of Engineering, Osaka University, 1-1 Yamadaoka, Suita, Osaka 565-0871, Japan, [c]Molecular Biology Research Center, Quantum Beam Science Directorate, Japan Atomic Energy Agency, 2-4 Shirakata-shirane, Tokai, Ibaraki 319-1195, Japan, and [d]Microbial Genome Research Group, Japan Agency of Marine-Earth Science and Technology, 2-15 Natsushima, Yokosuka, Kanagawa 237-0061, Japan

Correspondence e-mail: tamada.taro@jaea.go.jp, nojiri@ch.wani.osaka-u.ac.jp

The soluble region (residues 32–354) of GK0767, a copper-containing nitrite reductase from the thermophilic Gram-positive bacterium *Geobacillus kaustophilus* HTA426, has been cloned and overexpressed in *Escherichia coli*. The purified recombinant protein was crystallized using the hanging-drop vapour-diffusion method. X-ray diffraction data were collected and processed to a maximum resolution of 1.3 Å. The crystals belonged to space group $R3$, with unit-cell parameters $a = b = 115.1$, $c = 87.5$ Å. Preliminary studies and molecular-replacement calculations reveal the presence of one subunit of the homotrimeric structure in the asymmetric unit; this corresponds to a V_M value of 3.14 $\text{Å}^3\,\text{Da}^{-1}$.

1. Introduction

Denitrification, known as an example of anaerobic respiration, is a process in which nitrogenous compounds are used as alternative electron acceptors for energy production in living cells (Knowles, 1982). Recent earth-science and geochemical studies have revealed that the process contributes to the greenhouse effect and destruction of the ozone layer and it is also the major process for the return of fixed nitrogen to the atmosphere (Zumft, 1997). Complete denitrification involves four reaction steps ($NO_3^- \rightarrow NO_2^- \rightarrow NO \rightarrow N_2O \rightarrow N_2$) catalyzed by nitrate reductase, nitrite reductase, nitric oxide reductase and nitrous oxide reductase, respectively. One-electron reduction of NO_2^- to NO by nitrite reductase has been focused on as a key step in the denitrification process because this is the first step that leads to the gaseous products NO, N_2O and N_2.

Geobacillus is a phenotypically and phylogenetically coherent genus of thermophilic bacilli with high 16S rRNA sequence similarity (98.5–99.2%) and was separated from the genus *Bacillus* (Nazina *et al.*, 2001). Members of *Geobacillus* have been isolated from various terrestrial and marine environments not only in geothermal areas but also in temperate regions and permanently cold habitats (McMullan *et al.*, 2004), demonstrating a great capability for adaptation to a wide variety of environmental niches. *G. kaustophilus* HTA426, which was isolated from deep-sea sediment in the Mariana Trench, is a thermophilic organism of immense research interest. It grows optimally at 333 K, with an upper temperature limit of 347 K (Takami *et al.*, 1997; Takami, Nishi *et al.*, 2004). Its complete genome sequence has been reported as the first example of a thermophilic *Bacillus*-related species and is composed of a 3.54 Mb chromosome and a 47.9 kb plasmid (Takami, Takaki *et al.*, 2004). Meanwhile, *G. thermodenitrificans* is a facultative aerobe that is capable of growth by denitrification (Manachini *et al.*, 2000). Recently, genomic study of denitrifying *G. thermodenitrificans* NG80-2 has revealed the presence of complete gene clusters for denitrification: the first example in a Gram-positive bacterium (Feng *et al.*, 2007). The genome sizes and structures are quite similar in these two *Geobacillus* strains. The 2578 (74.9% of total putative proteins) NG80-2 genes have orthologues with an average protein identity of 83.2% in *G. kaustophilus* HTA426 and genome-wide synteny of orthologues between the two strains has also been detected (Feng *et al.*, 2007).

The amino-acid sequence deduced from the *nirK* gene (GK0767) encoding copper-containing nitrite reductase (CuNIR) in *G. kausto-*
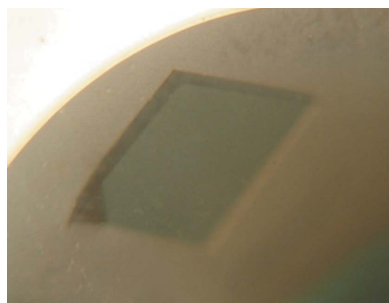
philus HTA426 shows extremely high similarity not only to GT0650 (96% identity) encoding NirK in *G. thermodenitrificans* NG80-2 but also to ADP75747.1 (82% identity) from *Geobacillus* sp. Y4.1MC1. However, the sequences also show relatively low similarities (~30%) to well known CuNIRs, although the residues in the Cu-binding sites and enzymatic functions are well conserved. This finding prompts speculation that *Geobacillus* CuNIRs commonly adapt to environmental stress by conformational changes arising from amino-acid replacements, deletions and/or insertions in the sequences. Moreover, a *ClustalW* alignment analysis (Thompson *et al.*, 1994) between *G. kaustophilus* CuNIR (*Gk*NIR), *Achromobacter xylosoxidans* CuNIR (*Ax*NIR; 19% identity to *Gk*NIR) as a class I CuNIR (Suzuki *et al.*, 1999) and *Neisseria gonorrhoeae* CuNIR (*Ng*NIR; 27% identity to *Gk*NIR) as a class II CuNIR (Boulanger & Murphy, 2002) reveals the presence of three characteristic loop regions in the amino-acid sequences of *Geobacillus* CuNIRs, which are named the 'linker loop', 'tower loop' and 'extra loop' in this study (Fig. 1). Therefore, determination and analysis of the three-dimensional structure of *Geobacillus* CuNIR is indispensable for a deeper understanding of the adaptive evolution of the CuNIR molecule at the atomic level.

Here, we describe the cloning, expression, purification, crystallization and preliminary X-ray analysis of GK0767, a copper-containing nitrite reductase from *G. kaustophilus* HTA426, as a first example of a *Geobacillus* CuNIR.

2. Experimental methods

### 2.1. Cloning, expression and purification

The gene encoding the putative soluble region from residues Glu32 to His354 of GK0767 was amplified by PCR using the genomic DNA of *G. kaustophilus* HTA426 as a template. The N-terminal region from Met1 to Ala31 was assumed to be a signal peptide for secretion using the amino-acid sequence-based prediction server *SignalP*3.0

(http://www.cbs.dtu.dk/services/SignalP/; Emanuelsson *et al.*, 2007). Moreover, the lipobox motif (Babu *et al.*, 2006) for the lipid-modified cysteine site (^{18}LAA^{21}C), which functions as an anchor to the cell membrane, was also found in this region. To identify whether this protein binds to the cell membrane using the putative lipid-modified site, it would probably be best to investigate the native form from the original growth culture. However, there was only a trace expression level under the cultivation conditions reported previously. Therefore, in this study the N-terminal region was deleted using a genetic engineering procedure for efficient overexpression in *Escherichia coli*. Sites for the restriction enzymes *Nde*I (CATATG) and *Hin*dIII (AAGCTT) were incorporated into the sequences of the forward and reverse primers, 5′-TA**CATATG**GAAAATAAAAACGGAACAG-CGGCAACTA-3′ and 5′-GG**AAGCTT**AATGTCCGCTTGTTTCT-GAGCCG-3′, respectively. The underlined parts of each sequence indicate the start and stop codons for amino-acid translation, respectively. The product DNA fragment was cloned into the T7 expression vector pET-20b(+) opened by digestion with *Nde*I and *Hin*dIII. The presence of the inserted gene was confirmed by DNA-sequence analysis. As a result, a Met residue originating from the vector was added at the N-terminus before the Glu32 residue of *Gk*NIR and the Glu residue was then numbered as the first residue in this study for clarity.

Plasmids for recombinant expression of *Gk*NIR were transformed into *E. coli* strain Rossetta-gami (DE3). 1.5 l Luria–Bertani medium containing 200 µg ml^{-1} ampicillin, 1.0 m*M* CuSO$_4$ and 4.0 mg ml^{-1} glucose was inoculated with colonies from a plate of the same medium cultured overnight at 310 K. The recombinant cells were incubated in the liquid medium for 24 h at 310 K. The cells were collected by centrifugation, washed with 40 m*M* Tris–HCl pH 8.0 (buffer *A*) containing 0.9%(*w/v*) NaCl and resuspended in 60 ml buffer *A* containing 1.0 m*M* CuSO$_4$ and 0.5 m*M* phenylmethylsulfonyl fluoride. The cells were disrupted by sonication in a chilled water bath and the cell lysate was incubated at 343 K for 30 min. The
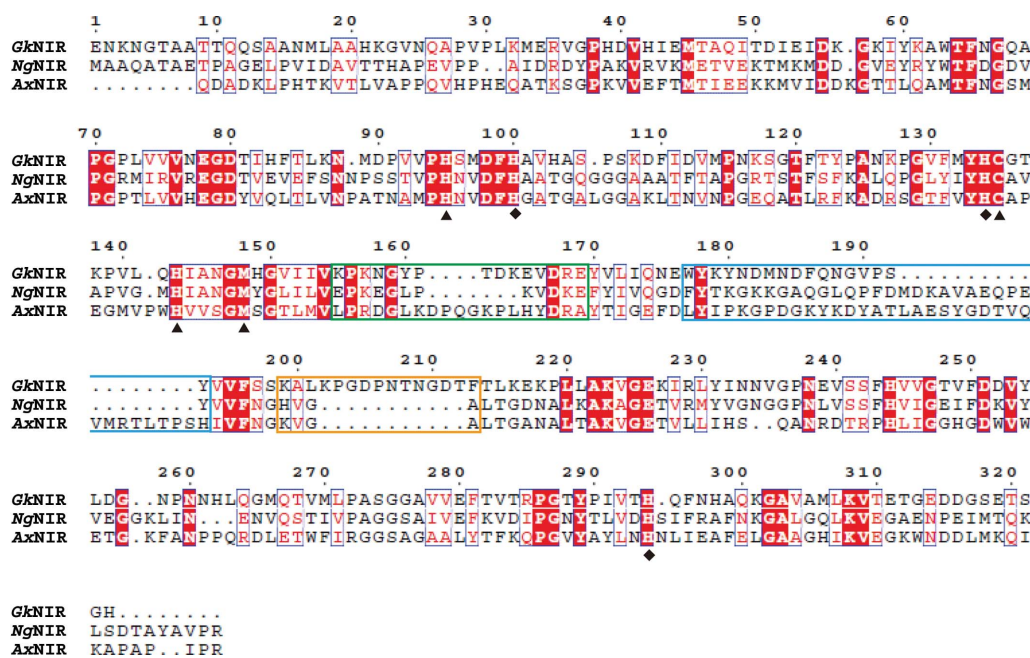
Figure 1
Sequence comparison between *Geobacillus* CuNIR and well known CuNIRs. Abbreviations and accession numbers are as follows: *Gk*NIR, GK0767 from *G. kaustophilus* strain HTA426 (gi:56419302); *Ng*NIR, CuNIR from *N. gonorrhoeae* strain FA1090 (gi:59718528); *Ax*NIR, CuNIR from *A. xylosoxidans* strain GIFU1051 (gi:3721763). *ClustalW* was used to perform sequence alignment (Thompson *et al.*, 1994) and the figure was generated using the program *ESPript* (Gouet *et al.*, 1999). Diamonds, type 1 Cu ligands; squares, type 2 Cu ligands. The three characteristic loop regions in *Gk*NIR are shown in coloured boxes: green, linker loop; blue, tower loop; orange, extra loop.
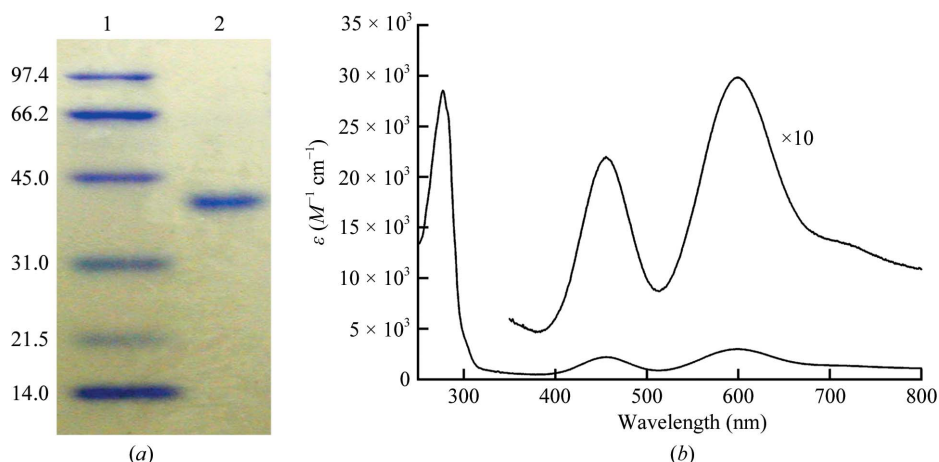
Figure 2
SDS–PAGE profile and UV–Vis absorption spectrum of the purified *Gk*NIR protein. (*a*) 12.5% SDS–PAGE. Lane 1, molecular-weight markers; the size of each protein (in kDa) is shown on the left. Lane 2, *Gk*NIR (3 µg). (*b*) UV–Vis absorption spectrum. The spectrum was measured in 40 m*M* Tris–HCl pH 8.0 at 298 K using a Shimadzu UV-2450 spectrophotometer. A 10× enlarged spectrum in the range 350–800 nm is also shown for clarity.

sample was centrifuged at 15 000*g* for 60 min and the supernatant was loaded onto a DEAE-Sepharose column (GE Healthcare UK Ltd, Buckinghamshire, England) pre-equilibrated with buffer *A*. After a wash with buffer *A*, the proteins were eluted with buffer *A* containing 0.2 *M* NaCl. The fractions containing *Gk*NIR were collected and a 40% saturated concentration of ammonium sulfate was added to the sample solution. After incubation at 277 K for 30 min, the solution was centrifuged at 15 000*g* for 30 min and the supernatant was loaded onto a Phenyl-Sepharose column (GE Healthcare UK Ltd, Buckinghamshire, England) pre-equilibrated with buffer *A* containing a 40% saturated concentration of ammonium sulfate. After elution with buffer *A*, the fractions containing *Gk*NIR were collected and dialysed with buffer *A* at 277 K for 12 h. The sample was loaded onto a Q-Sepharose column (GE Healthcare UK Ltd, Buckinghamshire, England) pre-equilibrated with buffer *A* and after a wash with buffer *A* containing 0.1 *M* NaCl the protein was eluted with a linear gradient of NaCl concentration from 0.1 to 0.2 *M*. *Gk*NIR was estimated to be >95% pure using SDS–PAGE; the absorption ratio (A_{280}/A_{600}) was 9.3 (Fig. 2).

2.2. Crystallization experiments

The protein was concentrated using a Millipore Centriprep-YM30 (30 kDa molecular-weight cutoff, Millipore, Massachusetts, USA). The protein concentration was determined by measuring the absorbance at 280 nm. A preliminary crystallization screen was carried out using Crystal Screen, Crystal Screen 2, MembFac and PEG/Ion kits (Hampton Research, California, USA). Hanging-drop vapour-diffusion experiments were set up by pipetting drops consisting of 1 µl protein solution (20 mg ml^{-1}) and 1 µl well solution at 277 K. After optimization of the best screening condition, X-ray diffraction-quality crystals were grown in hanging drops consisting of 3 µl protein solution (250 mg ml^{-1}) and 3 µl well solution and the drops were equilibrated against 0.3 ml well solution [0.1 *M* acetate buffer pH 4.6, 5.5%(*w*/*v*) PEG 4000 and 175 m*M* ZnSO$_4$] at 293 K. The approximate dimensions of the *Gk*NIR crystals were 0.7 × 1.0 × 0.2 mm (Fig. 3).

2.3. Data collection and processing

Prior to synchrotron data collection, the crystals were rinsed with well solution containing 29.5%(*v*/*v*) 2-methyl-2,4-pentanediol as a cryoprotectant and then flash-cooled by immersion in liquid nitrogen. A data set was collected from a single crystal at 100 K on beamline BL38B1 at SPring-8 (Hyogo, Japan) using an ADSC Quantum 210 CCD detector (Area Detector Systems Co., California, USA). The *HKL*-2000 package (Otwinowski & Minor, 1997) and *SCALA* (Evans, 2006) as implemented in the *CCP*4 package (Winn *et al.*, 2011) were used to reduce, integrate and scale the collected data. Crystallographic statistics of the data are summarized in Table 1.
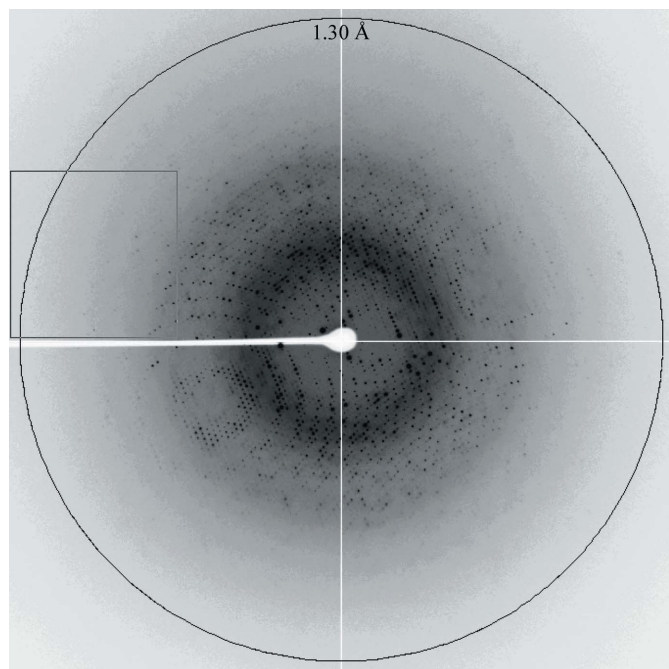
3. Results and discussion

The crystal diffracted to 1.3 Å resolution and belonged to the rhombohedral space group *R*3, with unit-cell parameters *a* = *b* = 115.1, *c* = 87.5 Å for the hexagonal cell (Fig. 4). Considering the molecular weight of *Gk*NIR (35 471 Da) and the cell volume (1 003 414.062 Å^3) and assuming the presence of one or two polypeptide chains of *Gk*NIR in the asymmetric unit, the calculated V_M values (Matthews, 1968) were 3.14 and 1.57 Å^3 Da^{-1}, corresponding to solvent contents of 60.9 and 21.8%, respectively.
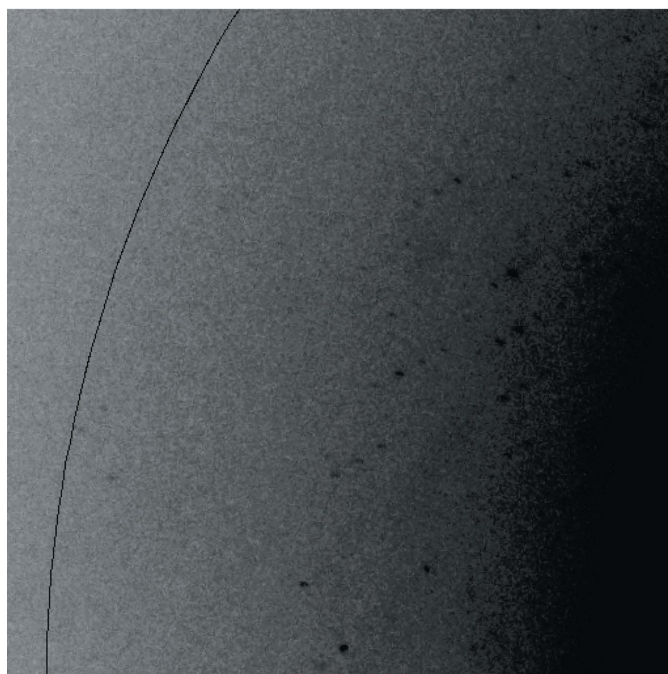
Molecular replacement with a monomeric subunit of *Ng*NIR (PDB entry 1kbw; Boulanger & Murphy, 2002) as a search model was performed in the resolution range 15.0–4.0 Å using *Phaser* (McCoy *et al.*, 2007), which gave only one solution, with a log-likelihood gain (LLG) of 69.5, in space group *R*3. Furthermore, a Patterson self-rotation calculation confirmed the absence of a crystallographic
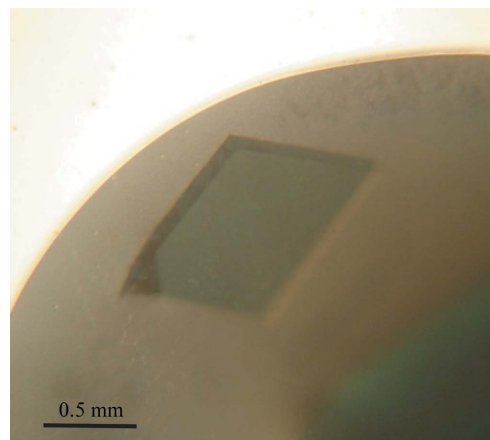
Figure 3
Crystal of *Gk*NIR. The crystal has approximate dimensions of 0.7 × 1.0 × 0.2 mm.

(a)

(b)

Figure 4
One-shot image of the diffraction pattern of a *Gk*NIR crystal. The pattern displays a maximum resolution of 1.3 Å and the crystal belongs to space group *R*3. (*a*) Overall image of one shot. (*b*) Enlargement of the inset box region of the overall image with adjusted background level for clarity.

Table 1
Crystal parameters and data-collection statistics for *Gk*NIR.

Values in parentheses are for the highest resolution shell.

Wavelength (Å)	1.0
Resolution (Å)	18.9–1.30 (1.37–1.30)
Space group	*R*3
Unit-cell parameters (Å)	$a = b = 115.1, c = 87.5$
R_{merge}†	0.080 (0.358)
$R_{p.i.m.}$‡	0.042 (0.256)
$\langle I/\sigma(I)\rangle$	14.9 (2.4)
No. of observations	356275 (33749)
No. of unique reflections	101119 (14139)
Completeness (%)	95.2 (90.8)
Multiplicity	3.5 (2.4)
Crystal mosaicity (°)	0.42

† $R_{merge} = \sum_{hkl}\sum_i |I_i(hkl) - \langle I(hkl)\rangle| / \sum_{hkl}\sum_i I_i(hkl)$, where $I_i(hkl)$ is the *i*th observation of reflection *hkl* and $\langle I(hkl)\rangle$ is the average intensity for all observations *i* of reflection *hkl*. ‡ $R_{p.i.m.} = \sum_{hkl}[1/(N-1)]^{1/2}\sum_i |I_i(hkl) - \langle I(hkl)\rangle| / \sum_{hkl}\sum_i I_i(hkl)$.

References

Babu, M. M., Priya, M. L., Selvan, A. T., Madera, M., Gough, J., Aravind, L. & Sankaran, K. (2006). *J. Bacteriol.* **188**, 2761–2773.

Boulanger, M. J. & Murphy, M. E. (2002). *J. Mol. Biol.* **315**, 1111–1127.

Emanuelsson, O., Brunak, S., von Heijne, G. & Nielsen, H. (2007). *Nature Protoc.* **2**, 953–971.

Emsley, P. & Cowtan, K. (2004). *Acta Cryst.* D**60**, 2126–2132.

Evans, P. (2006). *Acta Cryst.* D**62**, 72–82.

Feng, L., Wang, W., Cheng, J., Ren, Y., Zhao, G., Gao, C., Tang, Y., Liu, X., Han, W., Peng, X., Liu, R. & Wang, L. (2007). *Proc. Natl Acad. Sci. USA*, **104**, 5602–5607.

Gouet, P., Courcelle, E., Stuart, D. I. & Métoz, F. (1999). *Bioinformatics*, **15**, 305–308.

Knowles, R. (1982). *Microbiol. Rev.* **46**, 43–70.

Manachini, P. L., Mora, D., Nicastro, G., Parini, C., Stackebrandt, E., Pukall, R. & Fortina, M. G. (2000). *Int. J. Syst. Evol. Microbiol.* **50**, 1331–1337.

Matthews, B. W. (1968). *J. Mol. Biol.* **33**, 491–497.

McCoy, A. J., Grosse-Kunstleve, R. W., Adams, P. D., Winn, M. D., Storoni, L. C. & Read, R. J. (2007). *J. Appl. Cryst.* **40**, 658–674.

McMullan, G., Christie, J. M., Rahman, T. J., Banat, I. M., Ternan, N. G. & Marchant, R. (2004). *Biochem. Soc. Trans.* **32**, 214–217.

Murshudov, G. N., Vagin, A. A. & Dodson, E. J. (1997). *Acta Cryst.* D**53**, 240–255.

Nazina, T. N., Tourova, T. P., Poltaraus, A. B., Novikova, E. V., Grigoryan, A. A., Ivanova, A. E., Lysenko, A. M., Petrunyaka, V. V., Osipov, G. A., Belyaev, S. S. & Ivanov, M. V. (2001). *Int. J. Syst. Evol. Microbiol.* **51**, 433–446.

Otwinowski, Z. & Minor, W. (1997). *Methods Enzymol.* **276**, 307–326.

Suzuki, S., Kataoka, K., Yamaguchi, K., Inoue, T. & Kai, Y. (1999). *Coord. Chem. Rev.* **190–192**, 245–265.

Takami, H., Inoue, A., Fuji, F. & Horikoshi, K. (1997). *FEMS Microbiol. Lett.* **152**, 279–285.

Takami, H., Nishi, S., Lu, J., Shimamura, S. & Takaki, Y. (2004). *Extremophiles*, **8**, 351–356.

Takami, H., Takaki, Y., Chee, G.-J., Nishi, S., Shimamura, S., Suzuki, H., Matsui, S. & Uchiyama, I. (2004). *Nucleic Acids Res.* **32**, 6292–6303.

Thompson, J. D., Higgins, D. G. & Gibson, T. J. (1994). *Nucleic Acids Res.* **22**, 4673–4680.

Winn, M. D. *et al.* (2011). *Acta Cryst.* D**67**, 235–242.

Zumft, W. G. (1997). *Microbiol. Mol. Biol. Rev.* **61**, 533–616.

twofold-symmetry axis, which should be present if the space group was *R*32 and not *R*3. Interpretable electron density for the *Gk*NIR molecule was observed in difference Fourier $2F_o - F_c$ and $F_o - F_c$ maps calculated using phases from partial refinement of the *Gk*NIR model. Refinement using *REFMAC* (Murshudov *et al.*, 1997) and manual model building of the *Gk*NIR molecule using *Coot* (Emsley & Cowtan, 2004) are in progress.